

Radiopaque Polycaprolactone/Barium Sulfate Nanofibers for Applications in Soft Tissue Repair

Anna Marszałek^{1*}, Magda Kocyan¹, Tomasz Szwarec², Anna Ścisłowska-Czarnecka³, Agnieszka Królicka⁴, Marcin Gajek¹, Ewa Stodolak-Zych¹

¹Department of Biomaterials and Composites, AGH University of Krakow, Krakow, Poland

² Department of Swine and Small Animal Breeding, University of Agriculture in Krakow, Krakow, Poland

³ Institute of Applied Sciences, University School of Physical Education in Krakow, Krakow, Poland

⁴ Department of Building Materials Technology, AGH University of Krakow, Krakow, Poland

*Corresponding author: Anna Marszałek, Department of Biomaterials and Composites, AGH University of Krakow, Krakow, Poland amarszalek@agh.edu.pl

Submitted: 18th March 2025

Accepted: 9th June 2025

Abstract

Purpose: Monitoring performance of material inside the human body is still an open problem. X-ray imaging is easy and non-invasive method of visualization, however many biomaterials are radiolucent, such as polymers. Potential solution of this problem is to combine selected polymer with a compound which can act as a marker. Thus, this study aimed to obtain radiopaque polymeric fibers of polycaprolactone (PCL) by electrospinning.

Methods: As radiopaque marker barium sulfate (BaSO_4) powder was used. The obtained composite nonwovens were subjected to physicochemical properties (wettability, surface free energy), mechanical (uniaxial tensile test), stability in acidic environment and biocompatibility tests.

Results: Barium sulfate (of size 0,03-1,3 μm for non-grinded, 0,8-90 μm for grinded) was encapsulated inside the PCL fibers (average diameter 0,91 μm), proved by scanning electron microscopy observations and energy-dispersive X-ray spectroscopy. Addition of barium sulfate to the fibers in caused them to become thicker and changed diameter distribution from bimodal to unimodal. All materials were hydrophobic, with contact angle for water over 120° with no statistically significant difference and their surface free energy consisted mainly of disperse component (around 1:10 P/D ratio). Mechanical properties such as the maximum tensile force and tensile strength decreased by 50-60% after addition of barium sulfate. After three and seven days of cell culture with BJ fibroblasts, obtained materials proved to be biocompatible.

Conclusions: The results presented in this work allow to state that fibrous composite material composed of PCL and barium sulfate has potential as biomaterial that can be visualized and monitored after implantation using RTG imaging.

Keywords: Radiopacity, barium sulfate, polycaprolactone, electrospinning, polymer, monitoring, soft tissue, regeneration

1. Introduction

The development of medical imaging, which is the visual representation of physiological and pathological changes occurring in the body, has greatly increased the effectiveness of medical diagnosis. Among the techniques four groups can be distinguished, using various physical phenomena to create images: magnetic resonance imaging, gamma-scintigraphy, ultrasonography and methods utilizing X-ray, for example computed tomography [37]. Among those groups especially X-ray imaging has great potential as method for monitoring both performance and location of implanted materials (e.g. endovascular stents), as its commonly used in clinical practice thanks to being fast, reliable and non-invasive technique [20]. However,

like every method, X-ray imaging requires sufficient intensity of the signal to generate image which would allow to distinguish the object of interest from the surrounding tissue. Most polymer-based biomaterials cannot be visualized due to their low radiographic density, which is similar to soft tissues, such as muscle, epithelium, connective tissue and nervous tissue, because of a similar elemental composition (hydrogen, oxygen, carbon). Especially long-term implants made of flexible materials, which can easily change their shape (contrary to e.g. metallic endoprotheses) should be able to be observed non-invasively to ensure patient safety. Such devices are surgical meshes often used in treatment of injuries resulting from accidents, heart valves, artificial blood vessels, catheters (in neurology, ophthalmology, urology, cardiology). Many works related to monitoring of behavior of implanted materials focus on implants with electronic components, especially within the circulatory system [23]. Implants integrated with sensors enable real-time monitoring of minor changes before they become detectable by other methods, until when the damage is irreversible. Nevertheless, the issue of surveillance of implants such as meshes, etc. remains largely unexplored. This drawbacks resulted in increasing interest in designing polymers with suitable visibility [37], [24], [8], [25], [31], [11].

There are different approaches to obtain radiopaque polymers. Early studies were focused on physical mixtures of polymers and metals or inorganic salts, such as iodine, barium, bismuth, zircon and tantalum. However, those materials were not homogenous due to incompatibility of ionic salts and polymer matrix, which had negative effect on their mechanical properties [37], [24], [8]. The next stage of the search was the creation of single-phase mixture consisting of polymer-salt complex owing to the ability of some polymers to act as the ligands for chelation, avoiding modification of mechanical properties [24], [8]. Currently, the possibility of using various ceramic particles as radiopaque additive is studied, e.g. γ -Fe₂O₃, CaF, Y₃F or HAp, as well as organic compounds as indocyanide green, ioxinadol and iohexol [20], [25], [31].

The different approach is to introduce radiopaque monomeric units before polymerization, such as iodine compounds. There is no risk of leakage of radiopaque agent as it is permanently bound in the polymer. Unfortunately, synthesis of desired polymer can be complicated and ineffective. There is also not as wide a choice of polymer and contrast agent as with the first method, because this method is based on the homo- or copolymerization of iodine-containing monomers [20], [8], [2]. However, this method allows to easily obtain radiopaque nano- and microparticles using dispersion polymerization or precipitation of iodinated copolymeric chains. Microparticles can be used for visualization of embolization material and implants, while nanoparticles are useful in imaging of body organs and controlling behavior of nanoparticle-based drug delivery systems, since there is no risk of plugging blood

vessels, contrary to micrometer-sized particles. Contrast agents designed in this way ensure patient safety by preventing contact of radiopaque substance itself with the body [2].

Besides contrast agents used in diagnostic tests, when they are rapidly excreted, monitoring the biomaterial *in vivo* is particularly important for objects residing in the body for a long time, such as implants supporting the regeneration of damaged tissue. This application commonly uses polymers in fibrous form, as they imitate the microstructure of extracellular matrix [11], [39]. Incorporation of radiopaque marker can be easily accomplished by using the first of described approaches to obtaining radiopaque materials, i.e. mixing the appropriate substance with the polymer solution during the fiber manufacturing process using the selected method. As the result, fibers with encapsulated contrast agent are obtained [32]. The highest encapsulation efficiency is shown by studies where electrospinning is used to produce fibers. Additionally, it prevents thermosensitive compounds from degrading or changing structure and allows to produce fibers from various polymers such as proteins or carbohydrates, showing great potential in manufacturing complex and novel materials [32], [38].

Considering the need for radiopaque polymeric materials and taking in mind, that poly(ϵ -caprolactone) is one of the most commonly used for implantable devices, this work aims to provide fibrous material based on this polymer, which can be visualized using X-ray technique. PCL is a synthetic polymer used for developing fibrous scaffolds for repairing both hard and soft tissues, drug delivery systems, and bioresorbable surgical sutures due to its cytocompatibility and biodegradability in the physiological environment. Moreover, it can be easily processed into various forms, such as nanoparticles, microcapsules or fibers and its cost is relatively low. Compared to other degradable polymers its degradation time is long (2 to 4 years depending on the molecular weight), which makes the need to control its presence in the body even more important [39], [22]. While PCL by itself is most suited to the design of long-term implantable systems, in fiber form it has wider application. It has been investigated for use in drug delivery systems, absorbable sutures and scaffolds for tissue engineering [39], [3]. In this study barium sulfate was used as radiopaque marker. This inorganic salt has been used for many years as a radiocontrast agent in form of water suspension, improving visualization of the gastrointestinal tract. Usually it is not deposited within the walls of intestine, unless the mucosa is injured. It was also used as marker in some bone cements, but has been shown to leak into surrounding tissues. However, both older and recent studies proved this compound to be non-toxic in short term and low doses [40], [28]. Although both PCL and barium sulfate are widely used and their properties are well known, there is not much research done on their combination [11], [39], [3]. There are works concerning materials based on this polymer showing radiopacity, using various contrast agents, such as hydroxyapatite, zirconium oxide or iodine compounds [25], [31], [11], [10].

In this study we hypothesize that electrospinning will allow to successfully encapsulate barium sulfate. We aimed to compare three materials based on PCL fibers to determine their morphology, physicochemical and mechanical properties and cellular response of fibroblasts.

2. Materials and methods

2.1. Solution preparation and electrospinning

Polycaprolactone (PCL, Sigma-Adrich, Mw ~ 80 kDa) was selected for the fibers fabrication. The solvent system was dichlorometane (DCM, POCH) and dimethylformamide (DMF, POCH) in 7:3 ratio. As an radio-opaque marker barium sulfate powder (BaSO_4 , Nacalai Tesque, Mw=233.39 g/mol) was used. Viscosity-stable solution of PCL of concentration 12% (w/v) in solvent system of DCM and DMF in 7:3 ratio was prepared and placed on a magnetic stirrer for 24 hours. Then BaSO_4 powder was mixed with polymer solution using ultrasonic processor (Vibra-Cell, Sonics Inc.). The electrospinning equipment able to stabilize humidity and temperature was used to obtain the fibers

The material was modified by adding 2% w/w BaSO_4 to the 12% w/v PCL solution. Two types of solutions were used: BaSO_4 was either used as-received (BaSO_4 NG) or after prior grinding (BaSO_4 G) using a ball mill for 1h with isopropanol as a medium. To study the effect of the amount of barium sulfate on the radiopacity of samples, 10 ml of a 12% w/v PCL solution in DCM/DMF (7:3) solvent system, containing 1%, 2%, 3%, 4% or 5% by weight, was prepared. The prepared solutions were homogenized with a ultrasonic homogenizer and poured onto dishes. The samples were placed under a fume hood for one week to allow the solvents to evaporate completely. Their ability to absorb the X-ray radiation was evaluated in order to select the optimal concentration of BaSO_4 using the X-ray equipment (XR 6000, GE Healthcare).

Table 1 Optimal electrospinning parameters

PCL concentration (w/v)	BaSO_4 concentration (w/v)	Solvent system	Voltage [kV]	Needle-collector distance [cm]	Flow rate [ml/h]
12%	2%	DMC/DMF (7:3)	14	9	2

2.2. Dynamic Light Scattering Method

Barium sulfate particles size distribution was measured using the laser light diffraction method (Mastersizer 2000, Malvern Instruments Ltd.). Distilled water with DISPEX dispersing agent (BASF SE) was used as the medium. The solution was homogenized for 5 minutes before testing. Tests were also carried out in DCM and DMF, as well as in solvent system DCM/DMF.

2.3. Scanning Electron Microscopy

The microstructure of barium sulfate powder and nonwoven materials were investigated by scanning electron microscopy (Apreo 2 SEM, ThermoFisher Scientific). Prior to observation, the samples were coated with a layer of carbon with a thickness of 6-10 nm. The SEM images of fibers were analyzed using ImageJ software (National Institute of Mental Health, v. 2015) to determine diameter size distribution. Energy-dispersive X-ray spectroscopy (EDS) was performed using the microscope to confirm the encapsulation of BaSO₄ powder in the fibers.

2.4. Physicochemical properties

Wettability of materials was determined through a sessile drop method using the goniometer (DSA 25 KRÜSS). Surface free energy was calculated based on contact angles for water and diiodomethane by Owens, Wendt, Rabel and Kaelble (OWRK) method, according to formula (1).

$$\gamma_{LV}(1 + \cos\theta) = 2 \left(\sqrt{(\gamma_{LV}^d \gamma_{SV}^d)} + \sqrt{(\gamma_{LV}^p \gamma_{SV}^p)} \right) \quad (1)$$

Where:

γ_{LV} – surface tension between liquid and gas [N/m]

γ_{SV} – surface tension between solid and gas [N/m]

θ – contact angle [°]

d and p respectively represent dispersion and polar interactions.

2.5. Porosity

Porosity was determined by gravimetric method. Circular samples with diameter of 1,6 cm were weighted and their thickness was measured. Apparent density of the materials was calculated according to formula (2).

$$\text{Apparent density of sample} = \frac{\text{mass of the sample}}{\text{surface area} \cdot \text{sample thickness}} \left[\frac{\text{g}}{\text{cm}^3} \right] \quad (2)$$

Then the porosity was calculated according to formula (3), assuming density for PCL = 1,145 g/cm³.

$$\text{Porosity} = \left(1 - \left(\frac{\text{Apparent density of sample}}{\text{Density of the material}} \right) \right) \cdot 100 [\%] \quad (3)$$

2.6. Optical profilometry

The nonwovens roughness and topography were evaluated using the Lext OLS 4000 laser confocal microscope (Olympus, Tokyo, Japan). The measurements were carried out on sample surfaces of 258 μm × 258 μm.

2.7. Mechanical testing

Values of nonwovens thickness required for mechanical tests were measured using ImageJ software (version 2015) on pictures taken with a digital optical microscope (VHX-900F Keyence). Universal testing machine (RetroLine 1435, ZwickRoell) was used to study the tensile strength of the nonwovens. Uniaxial tensile tests were performed at 5 mm/min on samples 0,5 cm wide and 6 cm long. Samples after 15 min, 30 min and 60 min of the electrospinning process were compared with each other. The effect of the addition of BaSO₄ particles on the tensile parameters of 60 min spun nonwovens was also investigated.

2.8. In vitro study

The *in vitro* study was divided into three steps. The first step involved 10-day incubation of the materials in an HCl solution of pH=2, simulating conditions in the stomach to study their stability in acidic environment. SEM images of the nonwovens after the incubation were taken. In the second step samples were incubated in 10 ml of distilled water or HCl solution for 7 days in 37°C to visually assess release of the additive from the fibers. The concentration of Ba²⁺ ions in distilled water and HCl after incubation was measured using flame photometry (BWB XP Flame Photometer). Then, cells-materials interactions were studied to ensure biocompatibility of substrates. For two time points four samples of each material were prepared and placed in tissue culture polystyrene (TCPS) 24-well plate. After sterilization with UV light, materials were seeded with $1 \cdot 10^4$ BJ fibroblasts and incubated at 37°C. Cell viability and toxicity of the samples were tested after 3 and 7 days of incubation using ViaLight BioAssay Kit (Lonza Bioscience) and ToxiLight BioAssay Kit (Lonza Bioscience) assays respectively. For luminescence measurement FLUOstar Omega (BMG Labtech) reader was used.

2.9. Ex vivo study

To study the effect of the barium sulfate additive on the radiopacity of the material, an X-ray machine was used (XR 6000, GE Healthcare). PCL films with different BaSO₄ concentration (1%, 2%, 3%, 4%, 5% by weight) were examined. To verify the visibility in tissues, an *ex vivo* experiment was performed by placing the samples within the pig's stomach.

2.10. Statistical analysis

For fiber diameter 250 measurements were performed. For nonwoven thickness, 10 measurements were taken and for in vitro tests 4 replicates were made. For wettability, SFE and mechanical testing three replicates were made. Where applicable, results were presented as mean value \pm standard deviation. One-way analysis of variance followed by Tukey-Kramer *post hoc* test were used to identify statistically significant differences with p-value less than 0,05. To determine effect size, Cohen's f was calculated.

3. Results

BaSO₄ salt was added to the polymer matrices as a contrast agent. The purpose of grinding was to reduce the diameter of the powder grains to ensure a more uniform distribution of the salt in the fibers. The concentration of 2% was chosen based on an examination of the dispersion in DCM and DMF forming the solvent system.

3.1. Barium sulfate powder characterization

Firstly, non-grinded and grinded barium sulfate were observed using SEM (Figure 1). Both types are varied in size and have a tendency to agglomerate, however in case of grinded particles there are no grains as large as non-grinded ones.

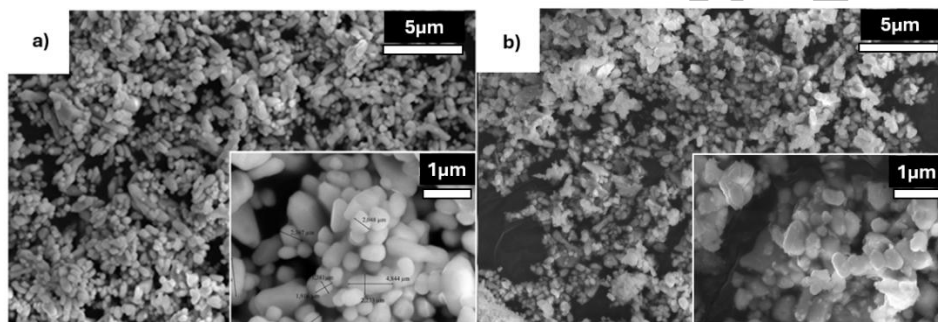


Fig. 1 SEM image of barium sulfate powder a) NG BaSO₄, b) G BaSO₄

Figure 2 compares distributions of size for particles of grinded and non-grinded BaSO₄, measured using DLS.

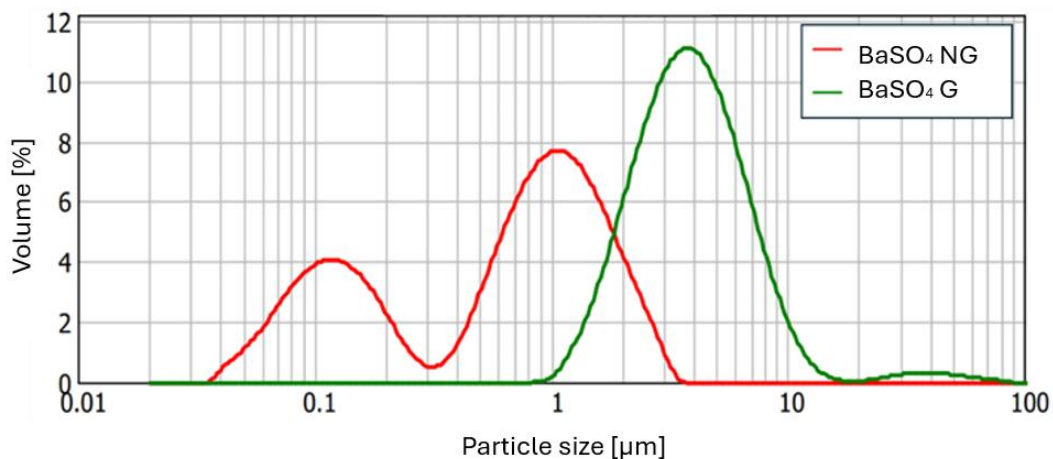


Fig. 2 Distribution of particles size for grinded and non-grinded barium sulfate

The behavior of barium sulfate particles in different solvents was also investigated to ensure stability of suspension. Figure 3 presents the results of the DLS measurements in the solvents used to prepare the spinning solution. Suspension of BaSO₄ particles in dimethylformamide

(DMF) is stable (Figure 3a), while in dichloromethane (DCM) the particles sediment rapidly (3b), thus it was impossible to perform repeatable measurements (three attempts are illustrated with different colors). The mixing of two solvents used as the solvent system used in the PCL electrospinning process prevents the particles from rapid precipitation and ensures the stability of the suspension (Figure 3c).

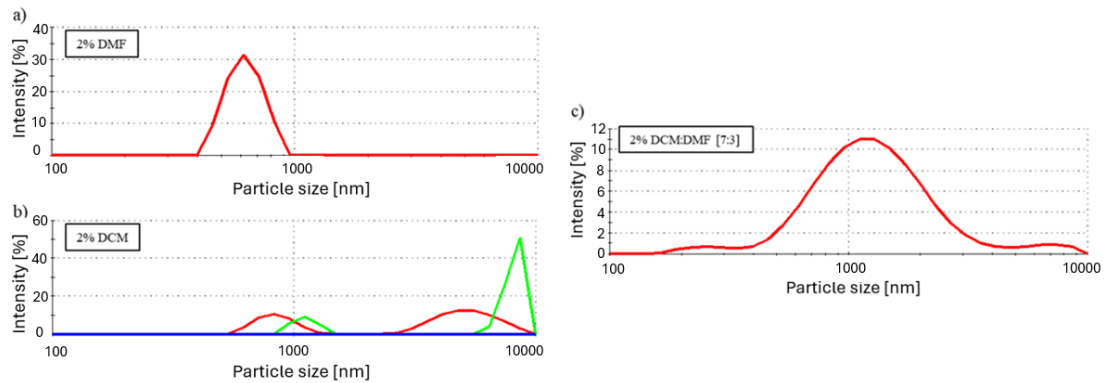


Fig. 3 BaSO₄ particles size measured in different media

3.2. Microstructure characterization

The obtained PCL nonwovens are characterized by a random orientation of fibers. 2 ml/h was picked as the optimum flow rate of the solution in the process of electrospinning, as it allows to obtain fibers of narrow bimodal distribution of diameter size and high surface smoothness. Figure 4 shows the microstructure of obtained materials observed using SEM. The fibers are free of beads and their diameter changes slightly along their length.

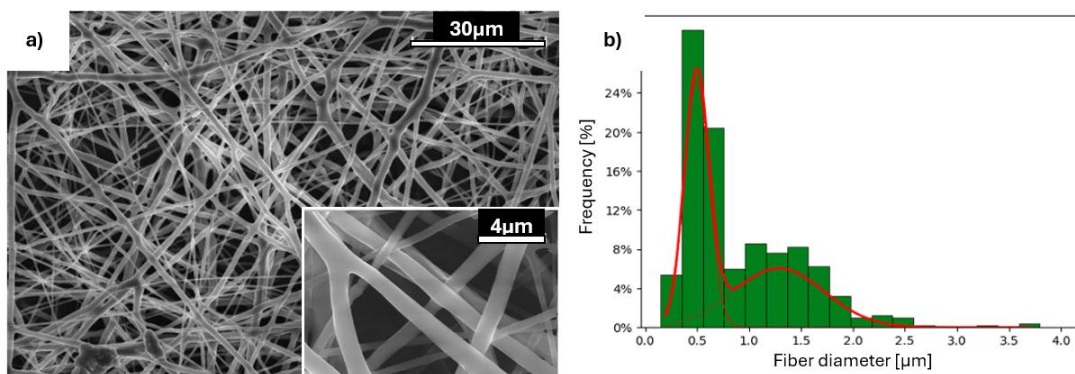


Fig. 4 Nonwoven consisting of PCL a) microstructure, b) fiber diameter distribution histogram

The effect of the addition of barium sulfate was studied by observing the microstructure of nonwovens. On Figure 5 comparison of PCL and composite fibers diameters ranges is presented. The addition caused the fibers to become more homogenous in diameter size - unlike in case of PCL fibers, the size distribution of PCL/BaSO₄ composite fibers is unimodal and shifted towards the higher values, as can be seen on Figure 6. That allows to draw the

conclusion, that addition of barium sulfate particles prevents forming fibers thinner than $0.94\ \mu\text{m}$ for PCL/BaSO₄ G and $0.42\ \mu\text{m}$ for PCL/BaSO₄ NG – meanwhile the thinner fibers for PCL have diameter of $0.18\ \mu\text{m}$. However, composite fiber also have lower spread of size – the thickest PCL have $3.72\ \mu\text{m}$, while none of composites have fibers thicker than $2.66\ \mu\text{m}$ and $2.76\ \mu\text{m}$ (BaSO₄ NG and G respectively). Table 2 contains additional statistical parameters calculated on the basis of diameters measurement.

On the SEM images, it can be observed how the barium sulfate is distributed inside and on the surface of the fibers. The particles form clusters of different sizes, irregular shapes and uneven distribution. In the case of grinded BaSO₄, the particles distribution is more homogeneous.

Figure 6c and 6f presents EDS spectra obtained for PCL/BaSO₄ nonwovens. The analysis shows characteristic peaks for sulfur and barium for both types of composite materials proving that barium sulfate has been successfully incorporated in the fibers [34].

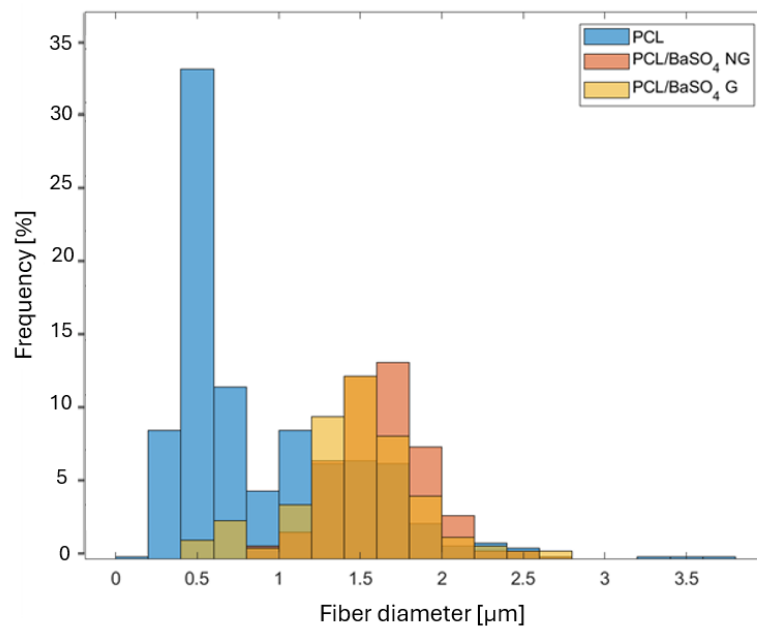


Fig. 5 Histograms showing comparison of fiber diameter distribution: PCL, PCL/BaSO₄ G and PCL/BaSO₄ NG

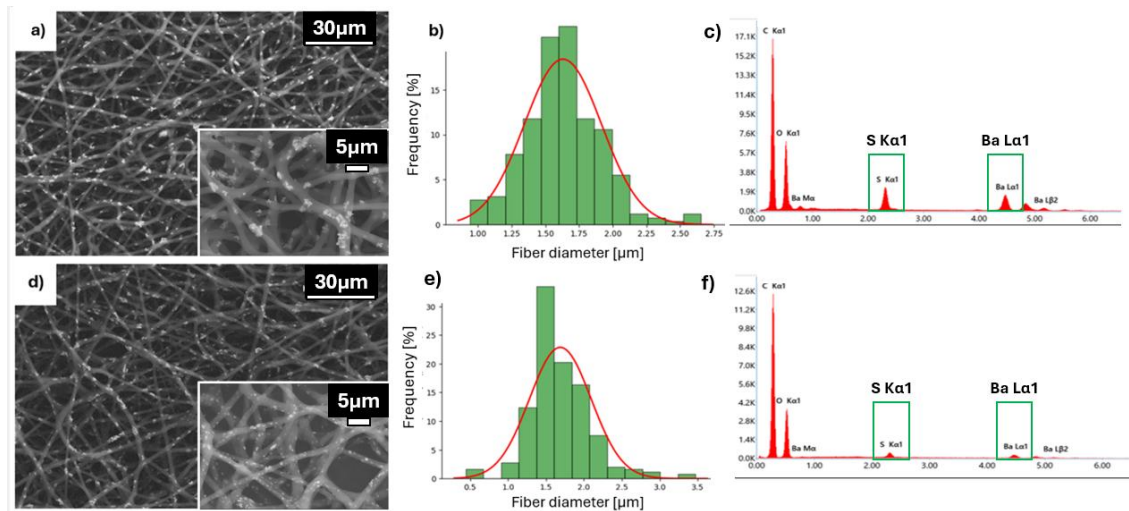


Fig. 6 PCL/BaSO₄ composite nonwovens; a, b, c) microstructure, fiber diameter distribution histogram and EDS spectrum for PCL/BaSO₄ NG; d, e, f) microstructure, fiber diameter distribution histogram and EDS spectrum for PCL/BaSO₄ G

Table 2 Calculated statistical parameters for morphology of the materials

Parameter		GROUP					
		PCL	NG	G	PCL x NG	PCL x G	NG x G
Fiber diameter [µm]		CI = [1.27 1.39]	CI = [1.60 1.67]	CI = [1.43 1.53]	p < 0.001* f = 0.38	p < 0.001* f = 0.17	p < 0.001* f = 0.22
Thickness [µm]	15 min	CI = [26.81 30.03]	CI = [16.23 18.44]	CI = [22.04 26.67]	p = 0.084 f = 2.49	p < 0.001* f = 0.64	p < 0.001* f = 1.20
	30 min	CI = [36.63 41.39]	CI = [20.73 25.73]	CI = [29.24 33.31]	p = 0.091 f = 2.20	p < 0.001* f = 1.08	p < 0.001* f = 1.24
	60 min	CI = [40.78 44.37]	CI = [21.09 25.57]	CI = [33.44 38.32]	p = 0.053 f = 2.94	p < 0.001* f = 11.19	p < 0.001* f = 1.66

3.3. Physicochemical properties

Measurements of contact angle with water of obtained materials confirmed that polycaprolactone is inherently hydrophobic polymer with contact angle for water over 90° [39], [22]. The value of contact angle is relatively small spread, indicating the uniformity of the surface in terms of wettability. Figure 7 compares contact angle for water on the studied materials. BaSO₄ has no significant effect on wettability, regardless of its form.

As expected of PCL, surface free energy consists mainly of dispersive component [6], [5]. Similarly to contact angle, BaSO₄ has no significant influence on SFE regardless of form.

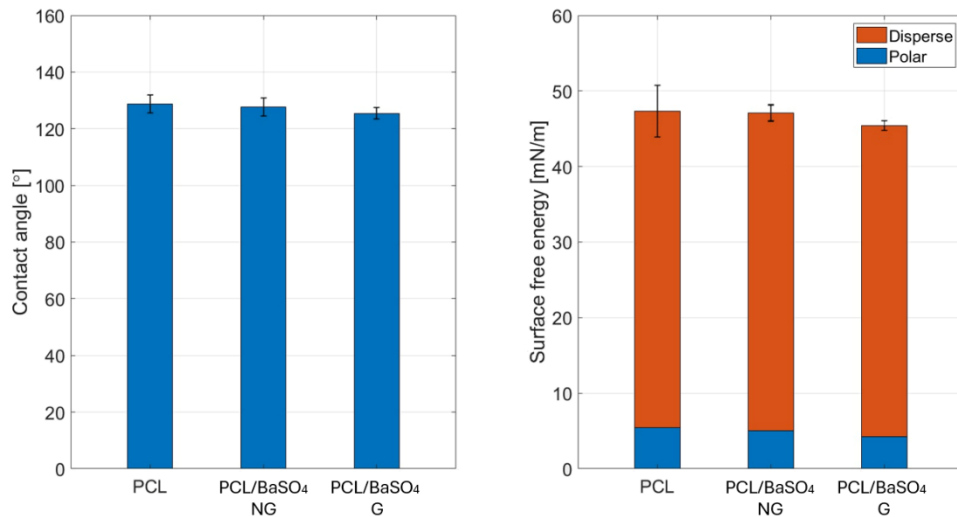


Fig. 7 Contact angle of PCL and PCL/BaSO₄ nonwovens

3.4. Porosity and profilometry

Table 3 shows porosity of produced non-wovens, higher than 90% regardless of composition. Both composite materials showed lower porosity than PCL. PCL/BaSO₄ G material was slightly less porous than PCL/BaSO₄ NG.

The results of 3D imaging using optical profilometer of the composite nonwovens are presented on Figure 8. Table 3 summarizes the roughness parameters of the surface profiles of the nonwovens: arithmetic average of profile height deviations from the mean line R_a , total height of the roughness profile R_t and quadratic mean of profile height deviations from the mean line R_q . There is significant difference between composite materials and PCL nonwoven for R_a , R_t and R_q parameters.

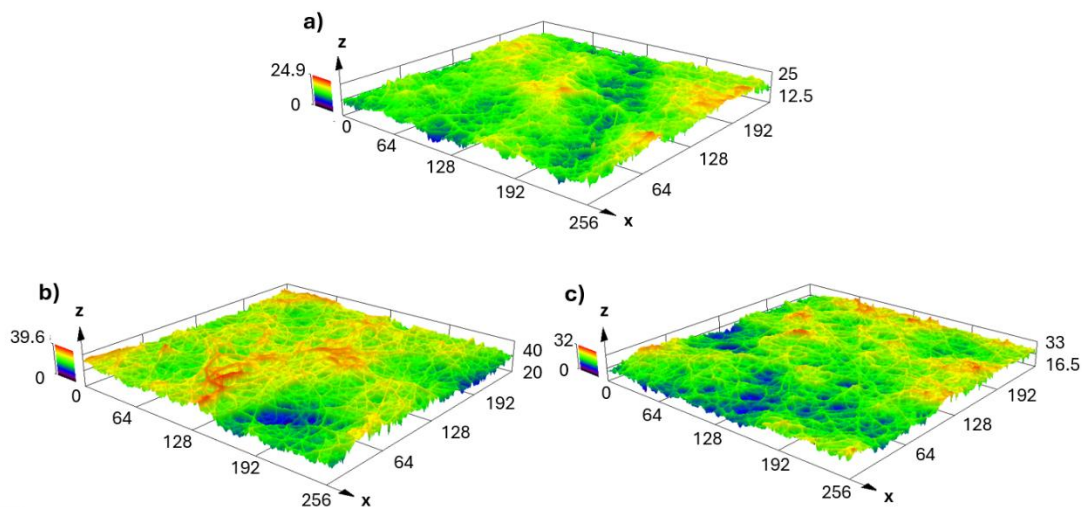


Fig. 8 Topography of surface of composite materials, a) PCL, b) PCL/BaSO₄ NG, c) PCL/BaSO₄ G

Table 3 Summary of physicochemical properties, size of fibers and roughness parameters

	PCL	PCL/BaSO ₄ (NG)	PCL/BaSO ₄ (G)
Contact angle [°]	128.75 ± 3.10	127.63 ± 3.16	125.44 ± 1.99
Total SFE [mN/m]	47.34 ± 4.71	47.06 ± 2.16	45.39 ± 1.87
Porosity [%]	95.12	93.28	91.92
Mean fiber diameter [μm]	0.91 ± 0.56	1.63 ± 0.29	1.48 ± 0.41
Fiber diameter range [μm]	0.18 – 3.72	0.94 – 2.66	0.42 – 2.76
R _a [μm]	1.91 ± 0.25	2.85±0.74	2.56±0.36
R _t [μm]	10.60 ± 3.20	17.20±3.98	16.10±2.09
R _q [μm]	2.37 ± 0.29	3.56±0.98	3.21±0.44

3.5. Mechanical testing

As thickness of the sample is necessary to calculate values of mechanical parameters such as tensile strength, in preparation to tensile testing thickness of the non-wovens was measured. Additionally, the effect of spinning time on thickness of the nonwovens was investigated. The results are presented as boxplots on Figure 9. Additional statistical parameters concerning the impact of time of the electrospinning process on the thickness of the material can be seen in Table 2.

Exemplary force-elongation curves obtained during tensile testing are shown on Figure 10. Table 4 summarizes measured and calculated parameters. Within the PCL nonwovens as well as PCL/BaSO₄ ones it is possible to observe analogous relationships – with an increase in thickness, the maximum tensile force (F_m) and tensile strength (σ) increase. In contrast, elongation at failure (ε_f) is highest for nonwovens spun for 30 minutes. The effect of the addition of barium sulfate on the mechanical parameters of nonwovens was investigated in uniaxial tensile test for different spinning times of nonwovens, in the same manner as for PCL nonwovens.

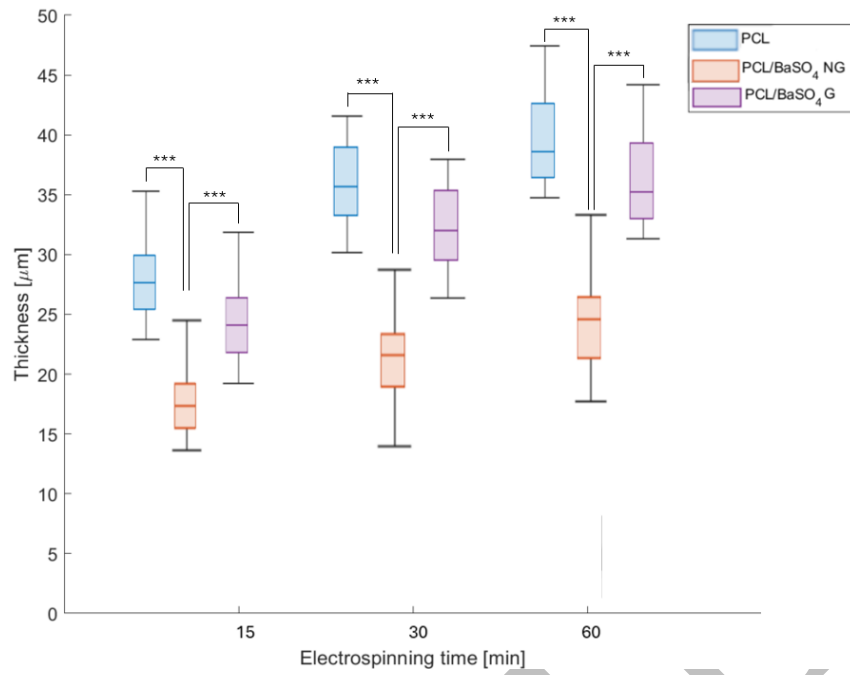


Fig. 9 Thickness of the nonwovens spun for various time

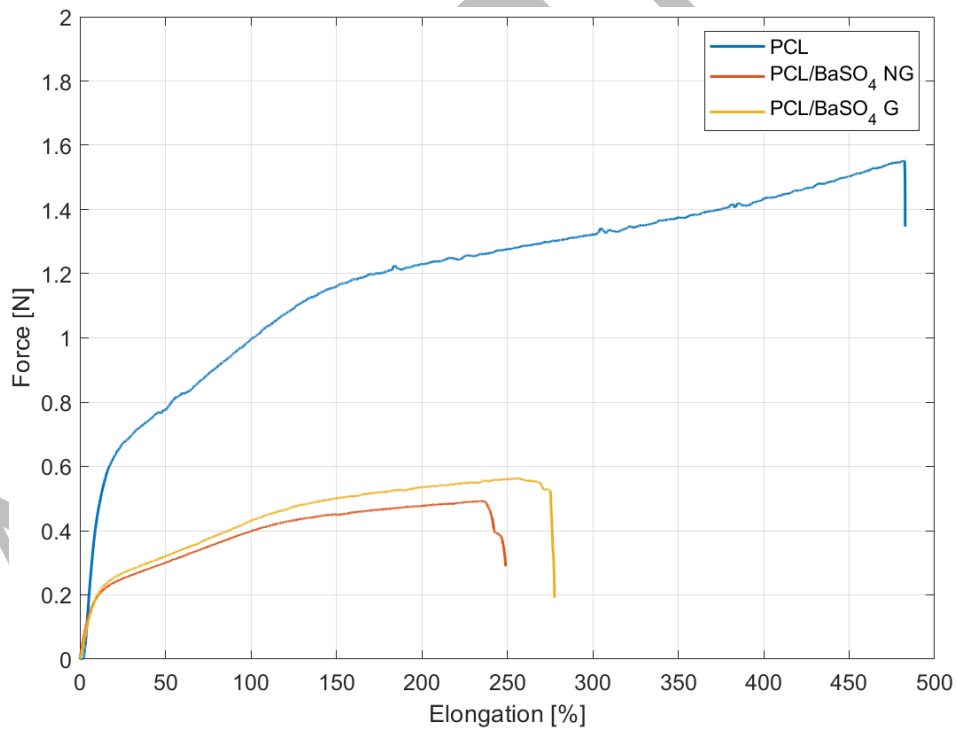


Fig. 10 Exemplary force-elongation curves for studied materials

Table 4 Summary of mechanical parameters of tested nonwovens

	Spinning time [min]	Maximum tensile force [N]	Ultimate strength [MPa]	Maximum elongation [mm]

PCL	15	0.276 ± 0.048	2.45 ± 0.43	135.30 ± 35.20
	30	0.559 ± 0.071	3.87 ± 0.50	168.10 ± 68.90
	60	1.190 ± 0.245	7.19 ± 1.48	139.60 ± 61.01
PCL/BaSO ₄ NG	15	0.148 ± 0.021	1.667 ± 0.24	164.36 ± 16.45
	30	0.279 ± 0.029	3.029 ± 0.27	176.46 ± 23.35
	60	0.542 ± 0.072	4.578 ± 0.73	122.81 ± 37.68
PCL/BaSO ₄ G	15	0.478 ± 0.057	0.425 ± 0.077	35.112 ± 5.48
	30	0.071 ± 0.012	0.491 ± 0.093	68.89 ± 12.54
	60	0.245 ± 0.343	1.480 ± 0.192	60.98 ± 7.26

3.6. In vitro study

The first stage of the in vitro study involved placing material samples in an HCl solution simulating the acidic environment of the stomach to examine the stability of the nonwoven under such conditions. Figure 11 presents SEM images of samples before and after the incubation in hydrochloric acid solution. They reveal changes in the in the microstructure of the nonwovens caused by acidic environment. A partial degradation of the fiber surface can be observed – the surface of the fibers after incubation is less smooth, and larger differences appear in the diameters of individual fibers along the length. However, despite visible changes in microstructure the material retained its integrity. Incubation in acidic environment caused the additive to release from the fiber surface in layers close to the surface of composite materials. In deeper layers, a few BaSO₄ grains remaining within the material can be observed.

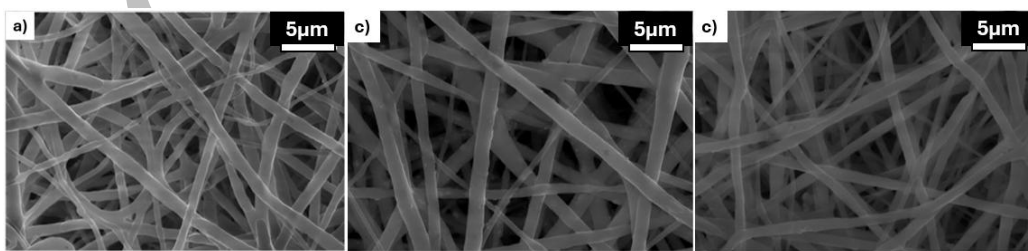


Fig. 11 Materials after incubation in HCl solution, a) PCL, b) PCL/BaSO₄ NG, c) PCL/BaSO₄ G

Then incubation in distilled water was performed. Figure 12 shows microstructure of the materials after incubation. The fibers are not degraded as when incubated in hydrochloric acid, and the additive was washed out to a lesser extent – grains are also visible in the fibers on the surface, especially for PCL/BaSO₄ G. Incubation of the obtained nonwoven fabrics with BaSO₄ in distilled water proved their stability. During this time, the release of barium sulfate occurred

in the near-surface layers. In contrast, the acidic environment caused the removal of the BaSO₄ additive from both composite materials. In addition, the concentration of barium ions in the solutions after incubation of the materials was determined. The results are shown in Table 5.

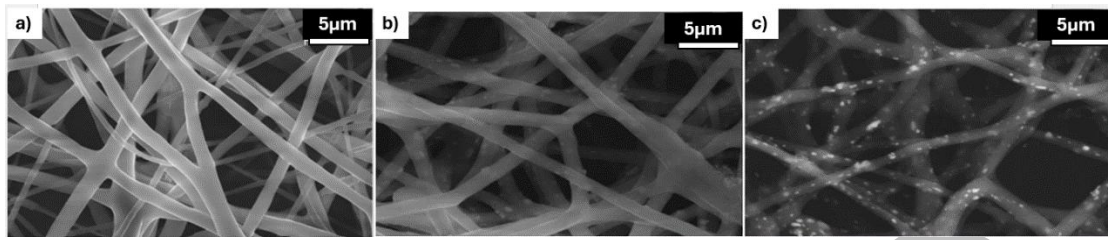


Fig. 12 Materials after incubation in distilled water, a) PCL, b) PCL/BaSO₄ NG, c) PCL/BaSO₄ G

Table 5 Concentration of Ba²⁺ ions after incubation

	PCL/BaSO ₄ NG		PCL/BaSO ₄ G	
	water	HCl	water	HCl
Ba ²⁺ concentration [mg/l]	21.2	40.5	21.5	38.2

Lastly, cell-material interaction was investigated. Figure 13 presents viability of BJ fibroblast after 3 and 7 days of culture. Higher value of ATP luminescence indicates greater amount of viable, metabolically active cells. For the tested materials, an increase of luminescence in time has been observed, suggesting that both PCL nonwoven and PCL/BaSO₄ composites are substrates allowing cells to proliferate on their surface. Comparison of PCL and PCL/BaSO₄ did not show significant difference, however the addition of grinded BaSO₄ had positive effect on the fibroblasts, improving their viability. Table 6 contains additional statistical parameters concerning in vitro testing.

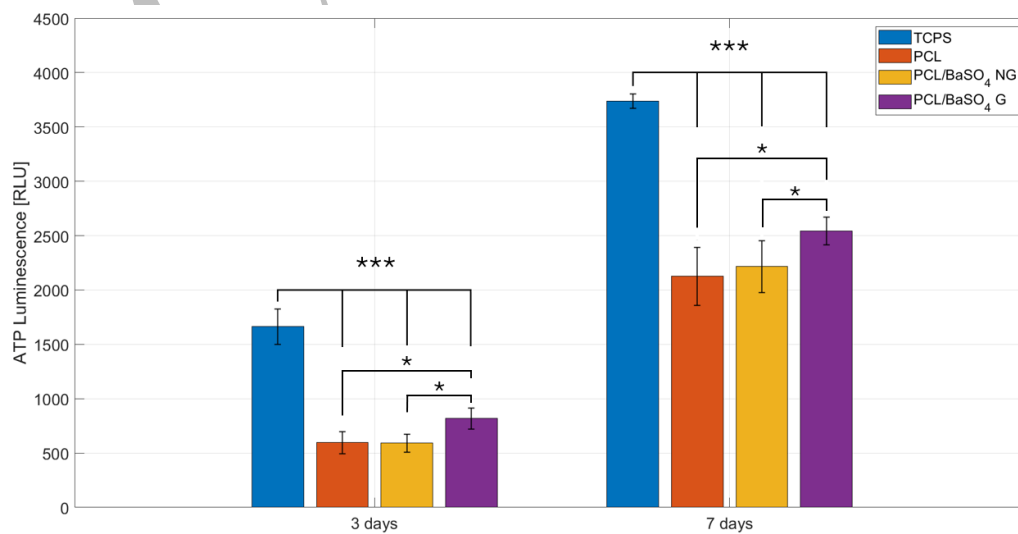


Fig. 13 Fibroblasts viability after 3 and 7 days of culture

Table 6 Calculated statistical parameters for in vitro tests results

Parameter		GROUP					
		PCL	NG	G	PCL x NG	PCL x G	NG x G
Viability	3 days	CI = [494.47 696.53]	CI = [507.95 672.55]	CI = [721.13 913.37]	p = 0.046* f = 0.03	p = 1.000 f = 0.78	p = 0.041* f = 0.88
	7 days	CI = [1863.10 2388.40]	CI = [1979.25 2450.25]	CI = [2416.18 2665.82]	p = 0.051 f = 0.699	p = 0.021* f = 0.124	p = 0.022* f = 0.599
Cytotoxicity	3 days	CI = [56.18 98.32]	CI = [112.65 130.85]	CI = [106.77 132.23]	p = 0.020* f = 0.95	p = 0.029* f = 0.841	p = 1.000 f = 0.07
	7 days	CI = [148.51 204.99]	CI = [248.26 378.24]	CI = [248.26 378.24]	p = 0.079* f = 2.045	p = 0.009* f = 0.944	p = 0.371 f = 0.364

A complementary cytotoxicity test was also performed (Figure 14). After 3 days, the toxicity of composite materials was slightly higher than for PCL fibers, but after 7 days the difference between them increased, composite materials showing higher cytotoxicity.

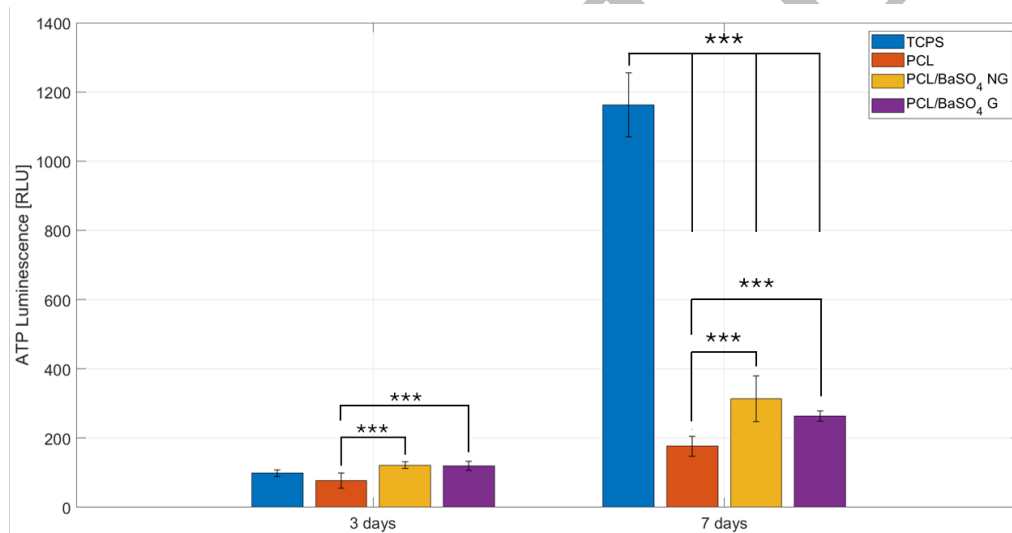


Fig. 14 Cytotoxicity of studied materials - after 3 and 7 days of culture

3.7. Ex vivo study

Figure 15. shows the pictures of composite films obtained with casting method with various BaSO₄ concentrations, obtained using X-ray equipment. RTG images of composite nonwovens were also taken during the *ex vivo* experiment (Figure 16).

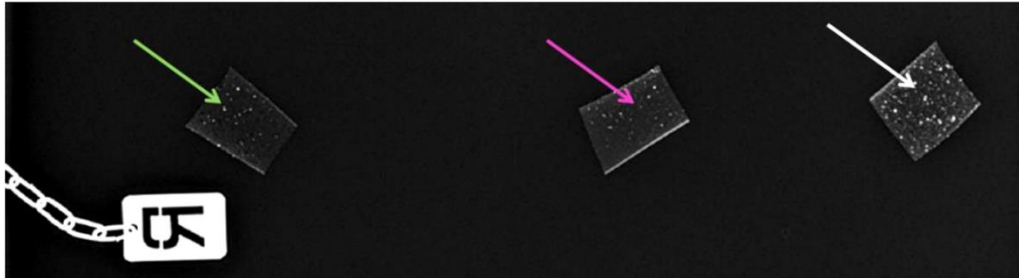


Fig. 15 RTG images of PCL films with barium sulfate added in different concentrations; sequentially from left 3%, 4%, 5%

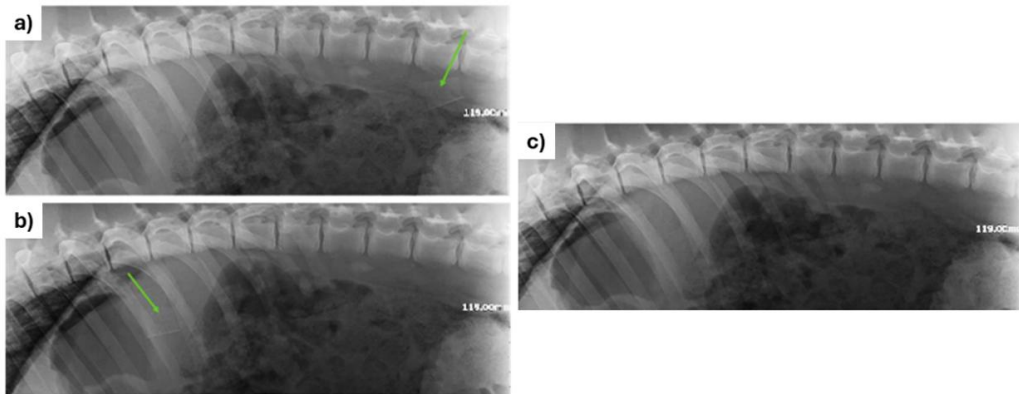


Fig. 16 RTG images in *ex vivo* experiment (abdominal cavity of pig); a) PCL/BaSO₄ 2%, non-grinded, b) PCL/BaSO₄ grinded, c) control

4. Discussion

4.1. Barium sulfate powder characterization

The particle size of non-grinded barium sulfate ranges from 0.03 μm to 1.3 μm and its distribution is bimodal, with the two most common values being approximately 0,1 μm and 1 μm . In the case of grinded BaSO₄, the particles size was spread in broader range of 0.8-90 μm , with a largest population size of 3.5 μm . DLS measurement proved them to be larger than non-grinded, contrary to visual observation on SEM image. Additionally, this distribution is unimodal. Higher values were observed due to easier agglomeration of grinded particles. In works, where BaSO₄ was used as a contrast agent in solid form as powder, the particle size was 0.5 μm [11], [10]. BaSO₄ NPs significantly vary in size depending on the method of obtaining

and precursors (2-190 nm). In case of obtaining NPs directly by milling bulk material it is not possible to precisely control size of the particles [17].

4.2. Microstructure characterization

The effect of the addition of barium sulfate was studied by observing the microstructure of nonwovens. The addition caused the fibers to become more homogenous in diameter size. Unlike in case of PCL fibers, the size distribution of PCL/BaSO₄ composite fibers is unimodal and shifted towards the higher values, as can be seen on Figure 6. That allows to draw the conclusion, that addition of barium sulfate particles prevents forming fibers thinner than 0.94 μm for PCL/BaSO₄ G and 0.42 μm for PCL/BaSO₄ NG – meanwhile the thinner fibers for PCL have diameter of 0.18 μm. Composite fiber also have lower spread of size – the thickest PCL have 3.72 μm, while none of composites have fibers thicker than 2.66 μm and 2.76 μm (BaSO₄ NG and G respectively). This confirms the general observation, that encapsulating substance in the fibers in order to obtain composites affects their diameter [4], [9].

4.3. Physicochemical properties

Additives can affect the wettability of composites, for example, changing the nature of the surface from hydrophobic to hydrophilic. Such effect in case of PCL fibers have chitin nanofibril or ZnO nanoparticles, mainly due to changes in the topography of the surface, which becomes more rough [13], [29]. However, in this study no significant effect on wettability and SFE was found, despite higher roughness parameters measured for composite materials.

4.4. Porosity and profilometry

Porosity is a determining factor of cells behavior. High porosity allows cell spreading and migration, as well as exchange of nutrients and metabolites. Low packing density of fibers improves cell viability, proliferation and infiltration [30]. Addition of BaSO₄ increased values of roughness parameters, suggesting that the surface is more irregular. For two types of composite materials values are similar regardless of the form of BaSO₄ and their difference is insignificant. Many authors have concluded that surface roughness has a significant impact on the mechanical properties of fibrous materials, especially composites. In the case of higher roughness, fibers separate from each other more easily, impairing mechanical properties of the material as the result. At this point it can be hypothesized, that composite materials will perform worse than PCL fibers in tensile strength test [16], [12].

4.5. Mechanical testing

With an increase of the electrospinning process the thickness of the nonwoven increases – both for PCL and PCL/BaSO₄ composites regardless of form of the addition. The increase in nonwoven thickness is not directly proportional to the spinning time, as it slows down with

time. The difference between PCL nonwoven and PCL/BaSO₄ composite is statistically insignificant, but there is a clear difference between PCL/BaSO₄ NG and two remaining materials. This suggests spinning process is hindered by the large grains, resulting in reduced efficiency. The reason may be changes caused by adding barium sulfate particles to the spinning solution, such as viscosity or conductivity. The effect of the addition of barium sulfate on the mechanical parameters of nonwovens was investigated in uniaxial tensile test for different spinning times of nonwovens, in the same manner as for PCL nonwovens. It can be seen that the addition of barium sulfate particles negatively affects the mechanical properties of the nonwovens (F_m , σ). This is the expected outcome, as various studies report, that encapsulation tends to impair the mechanical properties, especially the tensile strength of the material [20], [27]. However, the impact on mechanical properties strongly depends on the type of additive, concentration and size of the particles. For alternative radiopaque material such as hydroxyapatite, the addition as nanoparticles enhances such parameters as tensile strength, while introducing fibrous form improves the modulus of elasticity but impairs tensile strength due to agglomeration [15], [14]. In case of iodinated polymers, mechanical properties are strongly dependent on the structure and interactions between the chains [26], [33], [18]. In addition, the relationship between higher surface roughness and strength deterioration was confirmed [16], [12].

4.6. In vitro study

Acidic aqueous fluids are commonly present in living tissues favor the release of radiopaque salts. Besides potentially toxic effects, it gradually causes loss of the additive, changing the material into radiolucent [24]. The results presented in Table 5 confirm the release of the additive from the fibers with the ion concentration in the HCl solution being much higher. However, other works concluded, that neither BaSO₄ NPs nor Ba²⁺ ions significantly cross the intestinal barrier. If BaSO₄ NPs are orally administered, since the transit time in gastrointestinal tract is generally less than one day, 88% of them are removed within 24 hours. After 7 days almost 100% is removed from the body. Potential toxic effects of BaSO₄ are most likely concerning only the smallest particles (< 0.1 μ m), since they are more likely to pass to the bloodstream [1]. After that, barium sulfate nanoparticles localize mainly in the liver, spleen, bone marrow and lungs, with increasing accumulation in the bone. No evidence of genotoxicity in the bone marrow was found [19].

Analysis of viability and cytotoxicity makes it possible to select material with the most optimal biological properties. Various radiopaque additives have already been tested. Some of them, like zirconia [36] do not affect the properties of the material, while the other can promote cell growth e.g. nanostructured hydroxyapatite [35]. In case of iodinated polymers, which have

great potential as contrast agents, their impact on cells is still questionable. Extract from studied samples tend to be mildly cytotoxic in higher concentrations [33], [18].

All tested materials gave results indicating that the cells were viable and therefore the studied composites are biocompatible, pointing that the PCL/BaSO₄ is the most beneficial for cell growth. Since ECM contains hydrophilic species, it is important for the PCL material to be adequately modified to become more hydrophilic, as it promotes its interactions with the ECM. Higher wettability causes better cell adhesion and proliferation, which is the reason of various modification of inherently hydrophobic PCL, for example mixing appropriate additive into the spinning solution. In literature, there can be found reports of using peptides, small peptide sequences or hydrophilic polymers such as amino-functionalized tannin to improve the wettability of PCL fibrous materials [22], [5]. The produced composite materials did not change their wettability due to the addition of BaSO₄, as shown on Figure 7. and in Table 3, however they improved viability of fibroblasts comparing to PCL. This can be effect of increased roughness of the fibers surface, causing better adhesion of cells.

4.7. Ex vivo study

Larger agglomerates of the additive are more visible. Larger concentrations of BaSO₄ allow better, more detailed observation of the material. Tendency to increase visibility with increasing concentration was observed by authors studying various contrast agents, such as BaSO₄, other ceramic particles, like hydroxyapatite, baghdadite, zirconium oxide or organic compounds like indocyanine green [25], [31]. Different types of additives require different concentrations in the material to achieve satisfactory visibility in RTG imaging. Iodinated polymers are especially effective, as they do not require use of much iodine-containing compounds during synthesis [33], [18]. However, ceramic nanoparticles also have good visibility, as a few percent of hydroxyapatite or ZrO₂-Ba₂O₃ particles gives the material required visibility in X-ray, comparable to Al plate of a 1-5 mm thickness [21], [7]. RTG images of composite nonwovens taken during the *ex vivo* experiment (Figure 17) show that BaSO₄ concentration of 2% by weight is not sufficient to accurately determine the position of the material. Locating requires careful examination of the radiograph, and it can be difficult to determine the exact position of the nonwoven fabric against tissues. Minimally better visible on images is the composite containing non-grinded BaSO₄.

5. Conclusions

The results presented in this work allow to state that fibrous composite material composed of PCL and barium sulfate has potential as biomaterial that can be visualized and monitored after implantation using the most accessible imaging technique in medicine – RTG imaging. Addition

of BaSO₄ affects fiber diameter, surface roughness and mechanical properties, but does not change physicochemical properties of composites compared to PCL nonwovens. In distilled water the release of barium sulfate occurred in the near-surface layers. In contrast, the acidic environment removed BaSO₄ additive from all tested materials, causing degradation and deformations of fibers. Radiopacity was observed during *ex vivo* experiment for materials with 2 wt% BaSO₄, although higher concentration would be preferred for practical use.

Acknowledgments

Research project supported by program „Excellence Initiative – Research University” for the AGH University of Krakow (ID 4204).

References

- [1] Adolph W., Taplin G. V., Use of Micropulverized Barium Sulfate in X-Ray Diagnosis: A Preliminary Report, *Radiology*, 1950, 54(6):878–883, doi: 10.1148/54.6.878.
- [2] Aviv H., Bartling S., Kiesling F., Margel S., Radiopaque iodinated copolymeric nanoparticles for X-ray imaging applications, *Biomaterials*, 2009, 30(29):5610–5616, doi: 10.1016/j.biomaterials.2009.06.038.
- [3] Azimi B., Nourpanah P., Rabiee M., Arbab S., Poly (ε-caprolactone) Fiber: An Overview, *J. Eng. Fibers Fabr.*, 2014, 9(3), doi: 10.1177/155892501400900309.
- [4] Álvarez-Carrasco F. *et al.*, Development of Bioactive Hybrid Poly(lactic acid)/Poly(methyl methacrylate) (PLA/PMMA) Electrospun Fibers Functionalized with Bioglass Nanoparticles for Bone Tissue Engineering Applications, *IJMS*, 2024, 25(13):6843, doi: 10.3390/ijms25136843.
- [5] Causa F., Battista E., Della Moglie R., Guarnieri D., Iannone M., Netti P. A., Surface Investigation on Biomimetic Materials to Control Cell Adhesion: The Case of RGD Conjugation on PCL, *Langmuir*, 2010, 26(12):9875–9884, doi: 10.1021/la100207q.
- [6] Cava D., Gavara R., Lagarón J. M., Voelkel A., Surface characterization of poly(lactic acid) and polycaprolactone by inverse gas chromatography, *J. Chromatogr. A*, 2007, 1148(1):86–91, doi: 10.1016/j.chroma.2007.02.110.
- [7] Chen M.-S. *et al.*, Radiopacity performances of precipitated ZrO₂-doped Bi₂O₃ powders and the influences of dopant concentrations and sintering temperatures, *Ceram. Int.*, 2017, 43(16):14008–14014, doi: 10.1016/j.ceramint.2017.07.132.
- [8] Galperin A., Margel D., Baniel J., Dank G., Biton H., Margel S., Radiopaque iodinated polymeric nanoparticles for X-ray imaging applications, *Biomaterials*, 2007, 28(30):4461–4468, doi: 10.1016/j.biomaterials.2007.06.032.
- [9] Graciano Alvarez A. K. *et al.*, Electrospinning Poly(acrylonitrile) Containing Magnetite Nanoparticles: Influence of Magnetite Contents, *Fibers*, 2024, 12(3):19, doi: 10.3390/fib12030019.

- [10] Górecka Ż., Choińska E., Heljak M., Świążkowski W., Long-Term In Vitro Assessment of Biodegradable Radiopaque Composites for Fiducial Marker Fabrication, *IJMS*, 2022, 23(22):14363, doi: 10.3390/ijms232214363.
- [11] Górecka Ż. *et al.*, Biodegradable fiducial markers for X-ray imaging – soft tissue integration and biocompatibility, *J. Mater. Chem. B*, 2016, 4(34):5700–5712, doi: 10.1039/C6TB01001F.
- [12] Holmes J., Hafiz Y., Stachurski Z., Das R., Kalyanasundaram S., Surface topography evolution of woven thermoplastic composites under deformation, *Composites Part B: Engineering*, 2022, 188:107880, doi: 10.1016/j.compositesb.2020.107880.
- [13] Ji Y., Liang K., Shen X., Bowlin G. L., Electrospinning and characterization of chitin nanofibril/polycaprolactone nanocomposite fiber mats, *Carbohydr. Polym.*, 2014, 101:68–74, doi: 10.1016/j.carbpol.2013.09.012.
- [14] Karbowniczek J. E., Ura D. P., Stachewicz U., Nanoparticles distribution and agglomeration analysis in electrospun fiber based composites for desired mechanical performance of poly(3-hydroxybutyrate-co-3-hydroxyvalerate (PHBV) scaffolds with hydroxyapatite (HA) and titanium dioxide (TiO₂) towards medical applications, *Composites, Part B*, 2022, 241:110011, doi: 10.1016/j.compositesb.2022.110011.
- [15] Kasuga T., Ota Y., Nogami M., Abe Y., Preparation and mechanical properties of polylactic acid composites containing hydroxyapatite fibers, *Biomaterials*, 2001, 22(1):19-23, doi: 10.1016/S0142-9612(00)00091-0.
- [16] Kerans R. J., Jero P. D., Parthasarathy T. A., Issues in the control of fiber/matrix interfaces in ceramic composites, *Compos. Sci. Technol.*, 1994, 51(2):291–296, doi: 10.1016/0266-3538(94)90198-8.
- [17] Ketegenov T., Kamunur K., Batkal A., Gani D., Nadirov R., Recent Advances in the Preparation of Barium Sulfate Nanoparticles: A Mini-Review, *ChemEngineering*, 2022, 6(2):30, doi: 10.3390/chemengineering6020030.
- [18] Kiran S., James N. R., Joseph R., Jayakrishnan A., Synthesis and characterization of iodinated polyurethane with inherent radiopacity, *Biomaterials*, 2009, 30(29):5552–5559, doi: 10.1016/j.biomaterials.2009.06.049.
- [19] Konduru N. *et al.*, Biokinetics and effects of barium sulfate nanoparticles, *Part Fibre Toxicol*, 2014, 11(1):55, doi: 10.1186/s12989-014-0055-3.
- [20] Krufft M. A. B. *et al.*, Studies on two new radiopaque polymeric biomaterials, *J. Biomed. Mater. Res.*, 1994, 28(11):1259–1266, doi: 10.1002/jbm.820281103.
- [21] Leitune V. C. B., Collares F. M., Trommer R. M., Andrioli D. G., Bergmann C. P., Samuel S. M. W., The addition of nanostructured hydroxyapatite to an experimental adhesive resin, *J. Dent.*, 2013, 41(4):321-327, doi: 10.1016/j.jdent.2013.01.001.
- [22] Martins A. F. *et al.*, Novel poly(ϵ -caprolactone)/amino-functionalized tannin electrospun membranes as scaffolds for tissue engineering, *J. Colloid Interface Sci.*, 2018, 525:21–30, doi: 10.1016/j.jcis.2018.04.060.

- [23] Ma Y. *et al.*, Self-Powered, One-Stop, and Multifunctional Implantable Triboelectric Active Sensor for Real-Time Biomedical Monitoring, *Nano Lett.*, 2016, 16(10):6042–6051, doi: 10.1021/acs.nanolett.6b01968.
- [24] Mottu F., Rüfenacht D. A., Doelker E., Radiopaque Polymeric Materials for Medical Applications: Current Aspects of Biomaterial Research, *Invest. Radiol.*, 1999, 34(5):323, doi: 10.1097/00004424-199905000-00001.
- [25] No Y. J., Roohani-Esfahani S., Lu Z., Schaer T., Zreiqat H., Injectable radiopaque and bioactive polycaprolactone-ceramic composites for orthopedic augmentation, *J Biomed Mater Res*, 2015, 103(7):1465–1477, doi: 10.1002/jbm.b.33336.
- [26] Oyama Y., Kurokawa N., Hotta A., Multifunctionality of Iodinated Halogen-Bonded Polymer: Biodegradability, Radiopacity, Elasticity, Ductility, and Self-Healing Ability, *ACS Biomater. Sci. Eng.*, 2023, 9(11):6094–6102, doi: 10.1021/acsbiomaterials.3c01075.
- [27] Qi H., Hu P., Xu J., Wang A., Encapsulation of Drug Reservoirs in Fibers by Emulsion Electrospinning: Morphology Characterization and Preliminary Release Assessment, *Biomacromolecules*, 2006, 7(8):2327–2330, doi: 10.1021/bm060264z.
- [28] Rae T., Tolerance of mouse macrophages *in vitro* to barium sulfate used in orthopedic bone cement, *J. Biomed. Mater. Res.*, 1977, 11(6):839–846, doi: 10.1002/jbm.820110604.
- [29] Rivero P. J. *et al.*, Modeling Experimental Parameters for the Fabrication of Multifunctional Surfaces Composed of Electrospun PCL/ZnO-NPs Nanofibers, *Polymers*, 2021, 13(24):4312, doi: 10.3390/polym13244312.
- [30] Rnjak-Kovacina J. *et al.*, Tailoring the porosity and pore size of electrospun synthetic human elastin scaffolds for dermal tissue engineering, *Biomaterials*, 2011, 32(28):6729–6736, doi: 10.1016/j.biomaterials.2011.05.065.
- [31] Samuel R. *et al.*, Radiopaque poly(ϵ -caprolactone) as additive for X-ray imaging of temporary implantable medical devices, *RSC Adv.*, 2015, 5(102):84125–84133, doi: 10.1039/C5RA19488A.
- [32] Santos F. N. D. *et al.*, Antimicrobial activity of geranium (*Pelargonium graveolens*) essential oil and its encapsulation in carioca bean starch ultrafine fibers by electrospinning, *Int. J. Biol. Macromol.*, 2024, 265:130953, doi: 10.1016/j.ijbiomac.2024.130953.
- [33] Shiralizadeh S., Nasr-Isfahani H., Keivanloo A., Bakherad M., Yahyaei B., Pournali P., Preparation of radiopaque polyurethane–urea/graphene oxide nanocomposite using 4-(4-iodophenyl)-1,2,4-triazolidine-3,5-dione, *J Mater Sci*, 2018, 53(14):9896–9912, doi: 10.1007/s10853-018-2286-4.
- [34] Soundhirarajan P. *et al.*, Spectroscopic and non-spectroscopic analysis of Fe-substituted BaSO₄ nanoparticles by chemical precipitation method, *J Mater Sci: Mater Electron*, 2024, 35(19):1288, doi: 10.1007/s10854-024-13092-4.
- [35] Stastna E., Castkova K., Rahel J., Influence of Hydroxyapatite Nanoparticles and Surface Plasma Treatment on Bioactivity of Polycaprolactone Nanofibers, *Polymers*, 2020, 12(9):1877, doi: 10.3390/polym12091877.

[36] Thakare V. G., Joshi P. A., Godse R. R., Bhatkar V. B., Wadegaokar P. A., Omanwar S. K., Fabrication of polycaprolactone/zirconia nanofiber scaffolds using electrospinning technique, *J Polym Res*, 2017, 24(12):232, doi: 10.1007/s10965-017-1388-z.

[37] Torchilin V., Polymeric Contrast Agents for Medical Imaging”, *CPB*, 2000, 1(2):183–215, doi: 10.2174/1389201003378960.

[38] Wen P., Wen Y., Zong M.-H., Linhardt R. J., Wu H., Encapsulation of bioactive compound in electrospun fibers and its potential application, *J. Agric. Food Chem.*, 2017, 65(42):9161–9179, doi: 10.1021/acs.jafc.7b02956.

[39] Woodruff M. A., Hutmacher D. W., The return of a forgotten polymer— Polycaprolactone in the 21st century, *Progress in Polymer Science*, 2010, 35(10):1217–1256, doi: 10.1016/j.progpolymsci.2010.04.002.

[40] Zaccarini D. J., Lubin D., Sanyal S., Abraham J. L., Barium sulfate deposition in the gastrointestinal tract: review of the literature, *Diagn Pathol*, 2022, 17(1):99, doi: 10.1186/s13000-022-01283-8.

ACCEPTED